



MARCIN DZIADOSZ

Lublin University of Technology, Poland

ORCID iD: orcid.org/0000-0002-0506-6653

PIOTR BEDNARCZUK

WSEI University in Lublin, Poland

ORCID iD: orcid.org/0000-0003-1933-7183

ROBERT PIETRZYK

WSEI University in Lublin, Poland

ORCID iD: orcid.org/0000-0002-6837-4581

MARIUSZ SUTRYK

WSEI University in Lublin, Poland

ORCID iD: orcid.org/0000-0002-8998-125X

ADVANCED BLADDER ANALYSIS USING ULTRASONIC AND ELECTRICAL IMPEDANCE TOMOGRAPHY WITH MACHINE LEARNING ALGORITHMS

ZAAWANSOWANA ANALIZA
PĘCHERZA MOCZOWEGO
Z WYKORZYSTANIEM
ULTRADŹWIĘKOWEJ I ELEKTRYCZNEJ
TOMOGRAFII IMPEDANCYJNEJ
Z ALGORYTMAMI UCZENIA
MASZYNOWEGO

ABSTRACT

Purpose: The primary purpose of the study is to reconstruct the bladder based on the tomographic measurements obtained. Depending on the type of tomography used, two approaches are presented.

Methods: In the first presented case, the measurements were collected using ultrasonic tomography, while in the second one, they were gathered with electrical impedance tomography. Deterministic methods and machine learning algorithms, such as Elastic Net, Least Angle Regression, and a Neural Network, were used to obtain the bladder reconstruction.

Results: The bladder's position and size can be recognized based on the tomographic measurements of the UST and EIT. Both methods allow for its effective reconstruction.

Discussion: The research results are satisfactory, but their effectiveness is debatable. Future studies will focus on comparing and optimizing both solutions regarding reconstruction time.

STRESZCZENIE

Cel: Głównym celem przeprowadzonego badania jest otrzymanie rekonstrukcji pęcherza bazując na otrzymanych pomiarach tomograficznych. Przedstawione zostały dwa podejścia, w zależności od rodzaju zastosowanej tomografii.

Metody: W pierwszym prezentowanym przypadku pomiary zostały zebrane przy użyciu tomografii ultradźwiękowej, natomiast w drugim na podstawie elektrycznej tomografii impedancyjnej. Do otrzymania rekonstrukcji pęcherza zostały zastosowane metody deterministyczne i algorytmy uczenia maszynowego, takie jak Elastic Net, Least Angle Regression czy Sieć Neuronowa.

Wyniki: Na podstawie otrzymanych pomiarów tomograficznych UST i EIT możliwe jest rozpoznanie położenia oraz wielkości pęcherza. Obie zastosowane metody pozwalają na jego skuteczną rekonstrukcję.

Omówienie: Otrzymane rezultaty badania są zadowalające, jednak dyskusji podlega aspekt ich efektywności. Przyszłe prace będą skupione na porównaniu obu rozwiązań pod kątem czasu otrzymania rekonstrukcji oraz na ich optymalizacji.

KEYWORDS: *bladder analysis, tomographic measurements, machine learning, neural networks, reconstruction, ultrasonic tomography, electrical impedance tomography*

SŁOWA KLUCZOWE: *analiza pęcherza, pomiary tomograficzne, uczenie maszynowe, sieci neuronowe, rekonstrukcja, tomografia ultradźwiękowa, elektryczna tomografia impedancyjna*

INTRODUCTION

The urinary bladder is a vital organ in the human urinary system. It allows the storage of filtered urine and keeps it under control. The empty bladder has a pyramidal shape and fits into the pelvis. It becomes more spherical and moves into the abdominal cavity as it fills. It consists mainly of smooth muscle and connective tissue, which allows it to contract and expand under the pressure of accumulated urine. The bladder can hold from 400 to 700 ml of liquid. The kidneys produce urine and then flow down the ureters to the bladder, where it is stored. Once complete, the bladder is responsible for actively removing accumulated urine. For men, the bladder is higher than in women, in the pelvis, at the front of the rectum. The bottom of the bladder rests on the prostate gland. For women, the bladder is located in the pelvis, with the uterus located between it and the anus.

In medicine, tomographic imaging of the urinary bladder is essential for diagnosing, planning treatment, and monitoring the condition of this vital organ (Eimen et al., 2024; Peng et al., 2023). Accurate imaging of the urinary bladder's structure allows for detecting possible changes such as tumors, stones, or polyps. This will enable diseases to be diagnosed earlier, and appropriate treatment can be undertaken.

It is essential to monitor the organ's condition and detect possible abnormalities. Before bladder-related surgeries, such as stone removal or tumor resection, the tomographic image allows for precise procedure planning. The capacity, shape, and changes in the urinary bladder can be assessed. The doctor can see where exactly the problem is and how it relates to other anatomical structures. After a procedure or therapy, the image can be used to evaluate the effectiveness of treatment (Benfante et al., 2024; Kalinkina et al., 2024).

RESEARCH METHODOLOGY

Ultrasound tomography (UST), or ultrasonography, is a non-invasive imaging test using high-frequency sound waves (Dziodosz et al., 2024). UST is used in medicine to assess the internal structures of the patient's body and for examining abdominal organs (e.g., liver, kidneys, pancreas), thyroid gland, cardiovascular system, genitals, muscles, and joints (Kłosowski et al., 2023; Soleimani et al., 2024). During an ultrasound examination, a unique head emits sound waves reflected from internal tissues. An image of anatomical structures can be obtained based on the time it takes for the waves to return to the head. UST tomography is a safe method; it does not use ionizing radiation (unlike computed tomography or X-ray). It can be used for children, pregnant women, and the elderly. However, appropriate preparation may be required. For example, for an abdominal examination, the patient should be fasting.

Electrical impedance tomography (EIT) is a non-invasive medical imaging method that allows visualization of spatial distributions of conductivity and permittivity in the examined volume. EIT uses impedance measurement between surface electrodes surrounding the object. Different biological tissues are characterized by various values of electrical properties, which enable the reconstruction of tomographic images. EIT can also be used in many areas of medicine, such as diagnosing heart disease, monitoring the condition of soft tissues, or monitoring lung function. The respiratory cycle has a strong influence on conductance. During inspiration, lung tissue becomes more conductive due to less insulating air in the alveoli. EIT enables rapid visualization of regional lung ventilation, which is helpful in intensive care. It is also a safe method; it does not use ionizing radiation. It can treat children, pregnant women, and the elderly.

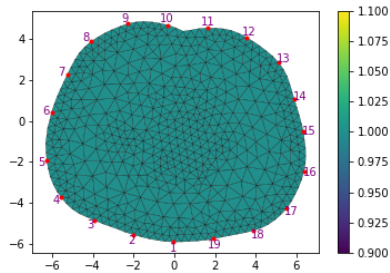
BLADDER RECONSTRUCTION USING ULTRASOUND TOMOGRAPHY

The research concerned a urinary tract phantom using ultrasonic tomography. Figure 1 presents a medical silicone phantom and the electrode placement points.

Figure 1. *Urinary system phantom*



For the reflection method, electrodes were applied to each point in turn, i.e., signal measurement was performed using ultrasonic transducers with different frequencies. The circumference of the phantom at the places where the electrodes are applied was 38 cm. The number of electrodes was 19. A mesh was made for the cross-section of the phantom at the electrode locations (Figure 2). Additionally, the electrodes were marked. There were 548 nodes and 999 finite elements.

Figure 2. *Cross-section grid*

Signals obtained from ultrasonic transducers with a frequency of 1 MHz were analyzed to determine the reflection moment. The reading frequency of the ultrasonic tomograph was 4MHz.

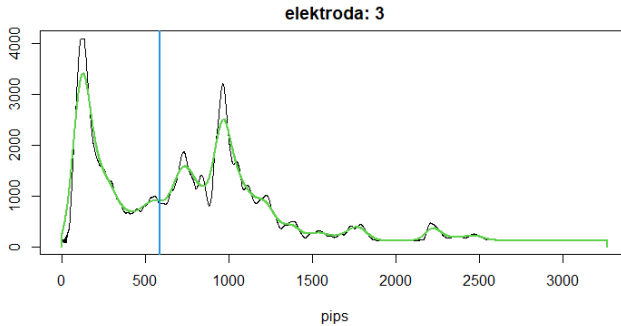
Figure 3. *Second wave detection (electrode 3)*

Figure 3 shows an exemplary analysis of the signal transmitted from electrode three and received from electrode 4. The peak of the second wave occurs at time 733, while the beginning occurs at time 587. Therefore, the transit time of the signal from the TX electrode to the edge of the bladder and back to the RX electrode is:

$$t = \frac{587}{4 \cdot 10^6} = 0.00014675 \text{ s} = 0.14675 \text{ ms.}$$

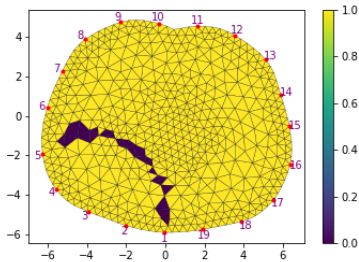
Depending on the speed of sound in medical silicone, the distance can be calculated as $d = vt$.

Bladder reconstruction was performed in two ways. For each pair of TX/RX electrodes, the reflection time of the second wave was determined, and then the path (the sum of the distances between TX and the bladder wall and RX and the bladder wall) of the signal was calculated. After determining the distance traveled, ellipse arcs were marked on the grid, with foci located in the places of the TX and RX electrodes. For example, for the speed of sound in medical silicone 540 m/s and the signal presented in Figure 3, the distance is equal to:

$$d = vt = 0.00014675s \cdot \frac{540m}{s} = 0.079245m = 7.9245cm.$$

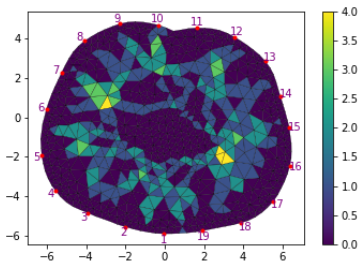
Figure 4 provides an example of such an arc on the grid.

Figure 4. Determining the arc of an ellipse



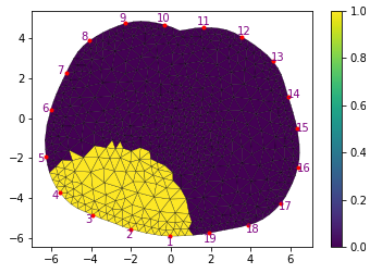
For each pair of electrodes, the arcs were placed on the grid (19 pieces), which resulted in the reconstruction of the bladder walls (Figure 6).

Figure 5. Reconstruction of the bladder edge



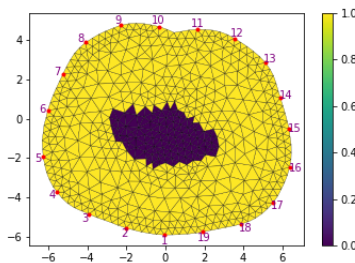
To reconstruct the bladder area, first, for each pair of TX/RX electrodes, it is essential to determine the area consisting of finite elements (Tolle and Marheineke, 2024; Zhang et al., 2024) for which the signal transit time from the TX electrode to the center of mass of the finite element and from the center of mass to RX exceeds the time until the start of the second wave (or the sum of the distances from electrode TX to the center of mass of the finite element and from the center of mass to RX exceeds the distance traveled by the signal in time to the beginning of the second wave reflection).

Figure 6. Determining the area of finite elements for which the sum of the distances of the component centers to the TX and RX electrodes exceeds the signal path until the second wave is reflected



In the next step, the standard part of the areas for each pair of electrodes was determined, thus obtaining a bladder reconstruction (Figure 7).

Figure 7. Reconstruction of the bladder area



BLADDER RECONSTRUCTION USING ELECTRICAL IMPEDANCE TOMOGRAPHY AND MACHINE LEARNING

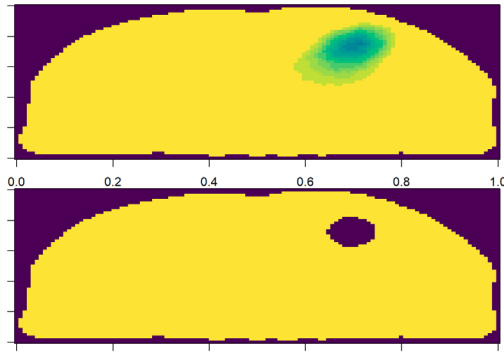
This chapter presents three machine learning algorithms (Elastic Net, Least Angle Regression, and a Neural Network with one hidden layer) used to obtain bladder reconstruction (Baran et al., 2023; Kulisz et al., 2024). Various sample size variants were considered to train the models, of which $\frac{3}{4}$ of the sample went to the training set and $\frac{1}{4}$ of the sample to the test set. An example comparison of the reconstruction and the real object is presented in each model case. The Mean Squared Error (MSE) was also calculated for each machine learning algorithm.

Elastic Net combines two popular variants of linear regression with regularization: ridge and lasso. It allows the use of both methods at the same time. The ridge variant uses L2 penalties to limit the values of the regression coefficients. It helps reduce the magnitude of the coefficients, which can prevent model overfitting. It is used when there are multiple collinear relationships between variables. On the other hand, the lasso type uses L1 penalties to reset some coefficients to zero. It helps in selecting important variables, eliminating those with less impact. Elastic Net combines both the L2 and L1 penalties. It allows for controlling the balance between L1 and L2 regularization (Allerbo et al., 2023; Chamlal et al., 2024; Merdas, 2024). The relationship between the number of cases in the training set and the quality of the obtained bladder reconstructions (measured as MSE) using the Elastic Net method is presented in Table 1. At the same time, Figure 8 compares the rebuilding and the real object.

Table 1. Relationship between the number of training cases and the quality of the bladder reconstructions – Elastic Net

Number of cases in the training dataset	MSE
75	0.0316511
750	0.0134917
1500	0.0130981
2250	0.0129405
3000	0.0130064
3750	0.0128988

Figure 8. Comparison of the reconstruction (the upper panel) and the actual object (the lower panel) – Elastic Net



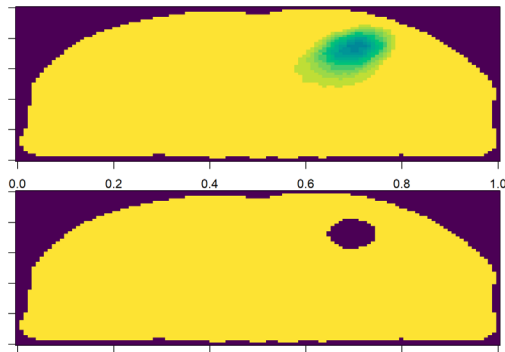
Least Angle Regression (LARS) is an algorithm used in statistics to fit linear regression models to high-dimensional data. It was developed by Bradley Efron, Trevor Hastie, Iain Johnstone, and Robert Tibshirani. It determines the solution path depending on the regularization parameter, showing how regularization affects the coefficients in the model. The algorithm iteratively selects the variables that have the most significant impact on the response and then targets those variables, minimizing the regression error. It resists multicollinearity (Allu and Padmanabhuni, 2023; An et al., 2023; Li et al., 2023).

Table 2 presents the relationship between the number of cases in the training set and the quality of the obtained bladder reconstructions (measured as MSE) using the Least Angle Regression method. At the same time, Figure 9 compares the rebuilding to the real object.

Table 2. Relationship between the number of training cases and the quality of the bladder reconstructions – LARS

Number of cases in the training dataset	MSE
75	0.0438626
750	0.0134724
1500	0.0130971
2250	0.0129209
3000	0.0131349
3750	0.0131125

Figure 9. Comparison of the reconstruction (the upper panel) and the actual object (the lower panel) – LARS



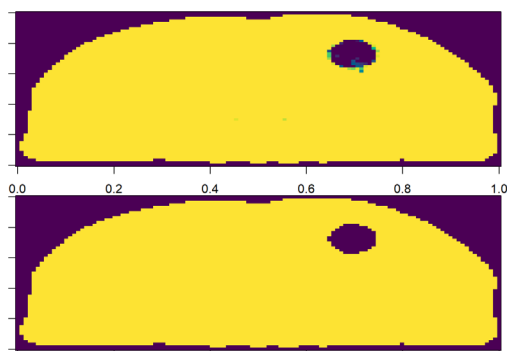
A neural network with one hidden layer consists of three main layers:

- an input layer that receives input data, e.g., image features, text or numbers,
- a hidden layer that consists of neurons that process input data. Each neuron computes a weighted sum of inputs and passes it through an activation function,
- an output layer that generates an output, such as image classification, weather forecast, or numerical value.

Neurons in the hidden and output layers use activation functions that introduce non-linearity into the model, which allows for more complex data transformations (Karakoyun, 2024; Xiao et al., 2024). The connection weights between neurons are initialized randomly. The network is trained on a training set, where the error is calculated for each example, and the weights are updated through backpropagation. The goal is to minimize errors in the training set and to be able to generalize to new data. It performs well in classification and regression problems (Bilokon, 2023; Hanif, 2024; Pan, 2024). The relationship between the number of cases in the training set and the quality of the obtained bladder reconstructions (measured as MSE) using the Neural Network method is presented in Table 3. At the same time, Figure 10 compares the rebuilding and the real object.

Table 3. Relationship between the number of training cases and the quality of the bladder reconstructions – Neural Network

Number of cases in the training dataset	MSE
75	0.0146815
750	0.0039885
1500	0.0026930
2250	0.0021705
3000	0.0020101
3750	0.0018679

Figure 10. Comparison of the reconstruction (the upper panel) and the actual object (the lower panel) – Neural Network

CONCLUSIONS

The study emphasizes the potential of non-invasive bladder detection and analysis techniques. Non-invasive imaging methods are the foundation of the success of modern medicine. These techniques do not require the insertion of instruments or penetration of the patient's body. This means there is no risk of tissue damage or infection. Patients also do not feel pain during non-invasive tests. This is important, especially in the diagnosis of children and people sensitive to pain. Additionally, these methods are relatively quick and convenient. Patients do not have to stay in hospital or undergo a long

convalescence process. Non-invasive imaging techniques can be used repeatedly without risk to the patient. However, it is worth remembering that each method has limitations and is not always suitable in every case. Depending on the patient's situation, the doctor will always select the most appropriate diagnostic method. Two approaches were presented – one based on ultrasound tomography and the second on electrical impedance tomography. Deterministic methods and machine learning algorithms were used to obtain the bladder reconstruction, delivering promising results.

Further work will focus on enhancing and optimizing the performance of the discussed methods. The resulting bladder reconstructions are already satisfying. However, improving their quality and shortening the time needed to obtain them is still possible.

REFERENCES

- Allerbo, O., Jonasson, J., Jörnsten, R. (2023). Elastic Gradient Descent, an Iterative Optimization Method Approximating the Solution Paths of the Elastic Net. *Journal of Machine Learning Research* 24, 1–53.
- Allu, R., Padmanabhuni, V. (2023). Convex Least Angle Regression Based LASSO Feature Selection and Swish Activation Function Model for Startup Survival Rate. *Cybernetics and Information Technologies* 23, 110–127. <https://doi.org/10.2478/cait-2023-0039>
- An, Y., Wang, H., Li, J., Li, G., Ma, X., Du, Y., Tian, J. (2023). Reconstruction Based on Adaptive Group Least Angle Regression for Fluorescence Molecular Tomography. *Biomedical Optics Express* 14. <https://doi.org/10.1364/BOE.486451>
- Baran, B., Kozłowski, E., Majerek, D., Rymarczyk, T., Soleimani, M., Wójcik, D. (2023). Application of Machine Learning Algorithms to the Discretization Problem in Wearable Electrical Tomography Imaging for Bladder Tracking. *Sensors* 23(3), 1553. <https://doi.org/10.3390/s23031553>
- Benfante, V., Salvaggio, G., Ali, M., Cutaia, G., Salvaggio, L., Salerno, S., Busè, G., Tulone, G., Pavan, N., Raimondo, D., Tuttolomondo, A., Simonato, A., Comelli, A. (2024). Grading and Staging of Bladder Tumors Using Radiomics Analysis in Magnetic Resonance Imaging. 93–103. https://doi.org/10.1007/978-3-031-51026-7_9
- Bilokon, O. (2023). Review and Analysis of the Development of Artificial Neural Networks. *Cybernetics and Computer Technologies* 68–80. <https://doi.org/10.34229/2707-451X.23.3.6>
- Chamlal, H., Benzmane, A., Ouaderhman, T. (2024). Elastic net-based high dimensional data selection for regression. *Expert Systems with Applications* 244. <https://doi.org/10.1016/j.eswa.2023.122958>
- Dziadosz, M., Mazurek, M., Hyka, O., Kowalski, M., Wójcik, D. (2024). Development and implementation of algorithms for measurement and reconstruction analysis in ultrasound tomography. *ELECTROTECHNICAL REVIEW* 1(4), 251–254. <https://doi.org/10.15199/48.2024.04.50>
- Eimen, R., Krzyzanowska, H., Scarpato, K., Ellerbee, A. (2024). Fiberscopic Pattern Removal for Optimal Coverage in 3D Bladder Reconstructions of Fiberscope Cystoscopy Videos. <https://doi.org/10.1101/2024.04.16.24305931>
- Hanif, D. (2024). Gauss-Newton Method for Feedforward Artificial Neural Networks.
- Kalinkina, O., Tezikov, Y., Lipatov, I., Mayorova, M., Sreseli, G. (2024). Analysis of a clinical case of managing a patient with intraoperative bladder injury. *Perm Medical Journal* 41, 148–153. <https://doi.org/10.17816/pmj411148-153>
- Karakoyun, M. (2024). Artificial neural network training using a multi selection artificial algae algorithm 53, 101684. <https://doi.org/10.1016/j.jestch.2024.101684>
- Kłosowski, G., Rymarczyk, T., Soleimani, M. (2023). Brain Sensing with Ultrasound Tomography and Deep Learning Algorithms, in: Proceedings of the 29th Annual

- International Conference on Mobile Computing and Networking. Association for Computing Machinery, New York, NY, USA, 1–3.
- Kulisz, M., Kłosowski, G., Rymarczyk, T., Słoniec, J., Gauda, K., Cwynar, W. (2024). Optimizing the Neural Network Loss Function in Electrical Tomography to Increase Energy Efficiency in Industrial Reactors. *Energies* 17(3), 681. <https://doi.org/10.3390/en17030681>
- Li, B., Wang, Y., Li, L., Liu, Y. (2023). Research on Apple Origins Classification Optimization Based on Least-Angle Regression in Instance Selection. *Agriculture* 13, 1868. <https://doi.org/10.3390/agriculture13101868>
- Merdas, H. (2024). Elastic Net – MLP – SMOTE (EMS) Based Model for Enhancing Stroke Prediction. *Medinformatics*. <https://doi.org/10.47852/bonviewME-DIN42022470>
- Pan, Y. (2024). Different Types of Neural Networks and Applications: Evidence from Feedforward, Convolutional and Recurrent Neural Networks. *Highlights in Science, Engineering and Technology* 85, 247–255. <https://doi.org/10.54097/6rn1wd81>
- Peng, Z., Shan, H., Yang, X., Li, S., Tang, D., Cao, Y., Shao, Q., Huo, W., Yang, Z. (2023). Weakly supervised learning-based 3D bladder reconstruction from 2D ultrasound images for bladder volume measurement. *Medical physics* 51. <https://doi.org/10.1002/mp.16638>
- Soleimani, M., Rymarczyk, T., Kłosowski, G. (2024). Ultrasound Brain Tomography: Comparison of Deep Learning and Deterministic Methods. *IEEE Transactions on Instrumentation and Measurement* 73, 1–12. <https://doi.org/10.1109/TIM.2023.3330229>
- Tolle, K., Marheineke, N. (2024). Nonlinear reduction using the extended group finite element method. *Computational and Applied Mathematics* 43, 1–18. <https://doi.org/10.1007/s40314-024-02637-2>
- Xiao, L., Zhang, Z., Huang, K., Jiang, J., Peng, Y. (2024). Noise Optimization in Artificial Neural Networks. *IEEE Transactions on Automation Science and Engineering* PP, 1–14. <https://doi.org/10.1109/TASE.2024.3384409>
- Zhang, Y., Ji, N., Wang, Z., Guo, C., Miao, X. (2024). Adaptive Finite Element Method for Magnetotelluric Forward Modeling with Gradient Recovery. <https://doi.org/10.21203/rs.3.rs-4084332/v1>